HHS Public Access

Author manuscript

Dev Biol. Author manuscript; available in PMC 2018 December 01.

Published in final edited form as:

Dev Biol. 2017 December 01; 432(1): 72–85. doi:10.1016/j.ydbio.2017.04.002.

Spop regulates Gli3 activity and Shh signaling in dorsoventral patterning of the mouse spinal cord

Hongchen Cai and **Aimin Liu***

Department of Biology, Eberly College of Science, Centers for Cellular Dynamics and Molecular Investigation of Neurological Disorders, Huck Institute of Life Sciences, The Pennsylvania State University, University Park, PA 16802, USA

Abstract

Sonic Hedgehog (Shh) signaling regulates the patterning of ventral spinal cord through the effector Gli family of transcription factors. Previous *in vitro* studies showed that an E3 ubiquitin ligase containing Speckle-type POZ protein (Spop) targets Gli2 and Gli3 for ubiquitination and degradation, but the role of Spop in Shh signaling and mammalian spinal cord patterning remains unknown. Here, we show that loss of *Spop* does not alter spinal cord patterning, but it suppresses the loss of floor plate and V3 interneuron phenotype of *Gli2* mutants, suggesting a negative role of Spop in Gli3 activator activity, Shh signaling and the specification of ventral cell fates in the spinal cord. This correlates with a moderate but significant increase in the level of Gli3 protein in the *Spop* mutant spinal cords. Furthermore, loss of *Spop* restores the maximal Shh pathway activation and ventral cell fate specification in the *Gli1;Sufu* double mutant spinal cord. Finally, we show that loss of *Spop-like* does not change the spinal cord patterning in either wild type or *Spop* mutants, suggesting that it does not compensate for the loss of *Spop* in Shh signaling and spinal cord patterning. Therefore, our results demonstrate a negative role of Spop in the level and activity of Gli3, Shh signaling and ventral spinal cord patterning.

Keywords

neural patterning; ubiquitin ligase; Gli1; Gli2; Sufu; Spopl

1. Introduction

Sonic hedgehog (Shh), a member of the family of Hedgehog (Hh) signaling proteins, plays a central role in the stereotypical arrangement of neural progenitors along the dorsal/ventral (D/V) axis of the ventral spinal cord in vertebrates (Briscoe and Therond, 2013). The Shh protein, produced in the notochord and subsequently in the floor plate, forms a ventral-to-dorsal gradient in the ventral spinal cord, and regulates the expression of a multitude of

*Author for correspondence. Aimin Liu, 201 Life Science Building, The Penn State University, University Park, PA 16802, USA. (814) 865-7043. AXL25@psu.edu.

target genes through a morphogen-like mechanism. These genes, mostly encoding transcription factors, subsequently interact with each other to form an intricate gene regulatory network that helps to sharpen the borders between them and define the locations of various groups of neural progenitors (Cohen et al., 2013).

The direct transcriptional responses to Shh are mediated by the effector Glioma-associated oncogene (Gli) family of transcription factors (Matise and Joyner, 1999). There are three Gli proteins in mammals, Gli1, 2 and 3. In the absence of Hh ligands, Gli2 and Gli3 are phosphorylated by PKA, CK2 and Gsk3, and are ubiquitinated by Cul1/β-TrCP ubiquitin ligase (Pan et al., 2006; Wang et al., 2000). The ubiquitinated Gli3 is partially degraded in the proteasome to produce a strong transcriptional repressor (Gli3R), whereas ubiquitinated Gli2 mostly undergoes complete degradation. Loss of Gli3 repressor activity results in ventralization of the forebrain and severe polydactyly in the limbs, but very subtle defects in the D/V patterning of the spinal cord, suggesting that the requirements for Gli3R activity vary dependent on the developmental contexts (Hui and Joyner, 1993; Persson et al., 2002; Theil et al., 1999; Tole et al., 2000).

Shh inhibits the Cul1/β-TrCP-based proteolytic processing of Gli3 and degradation of Gli2, and turns them into transcriptional activators (Gli2A and Gli3A) (Humke et al., 2010; Pan et al., 2006; Wang et al., 2000). Loss of *Gli2* results in the loss of floor plate and great reduction of V3 interneurons, ventral-most spinal cord cell types dependent on high concentrations of Shh, suggesting that Gli2 is the primary activator of the Shh pathway (Ding et al., 1998; Matise et al., 1998). Interestingly, loss of both *Gli2* and *Gli3* results in more complete loss of all floor plate and V3 interneurons, as well as the mixing of other ventral cell types including the motor neurons, V1 and V2 interneurons, suggesting that Gli3A also contributes to Shh pathway activation in the spinal cord (Bai et al., 2004; Lei et al., 2004). The third member of the Gli family, Gli1, whose transcription is dependent on Hh signaling, contributes to, but is not essential for, ventral spinal cord patterning (Bai et al., 2004; Park et al., 2000).

Suppressor of Fused (Sufu) inhibits Shh signaling and ventral spinal cord development in mammals (Cooper et al., 2005; Svard et al., 2006). *In vitro* studies suggested that Sufu represses Gli proteins both by sequestering them in the cytoplasm and by inhibiting Gli-mediated transcription in the nucleus (Barnfield et al., 2005; Cheng and Bishop, 2002; Ding et al., 1999; Dunaeva et al., 2003; Kogerman et al., 1999; Lin et al., 2014; Merchant et al., 2004; Murone et al., 2000; Paces-Fessy et al., 2004; Stone et al., 1999). Recent findings suggest that Hh signaling results in the primary cilium-dependent dissociation between Sufu and Gli proteins (Humke et al., 2010; Lin et al., 2014; Tukachinsky et al., 2010). Interestingly, we found that the floor plate and V3 interneurons failed to form in *Gli1;Sufu* double mutants, in striking contrast to normal spinal cord patterning in *Gli1* mutants, suggesting that Sufu is required for the maximal activation of Shh signaling in the absence of Gli1 (Bai et al., 2002; Liu et al., 2012; Park et al., 2000). This positive function of Sufu correlates with the observation that the levels of Gli2 and Gli3 proteins are greatly reduced in the absence of *Sufu*, suggesting that Sufu may promote Shh signaling by protecting the Gli proteins from degradation (Chen et al., 2009; Jia et al., 2009; Wang et al., 2010).

In addition to Cul1-based proteolytic processing, Gli2 and Gli3 are also subject to degradation mediated by a ubiquitin ligase containing Cul3 and Speckle-type POZ protein (Spop) (Chen et al., 2009; Wang et al., 2010; Wen et al., 2010; Zhang et al., 2009; Zhang et al., 2006). It was reported that Spop specifically targeted activated Gli3 for degradation (Wen et al., 2010), which appears to be consistent with reports suggesting antagonistic roles of Sufu and Spop in Gli2 and Gli3 degradation (Chen et al., 2009; Wang et al., 2010). These *in vitro* studies raised the possibility that Spop may be responsible for the great reduction in the levels of Gli2 and Gli3 in *Sufu* mutants. However, the *in vivo* roles of Spop in Shh signaling and spinal cord development, especially its role in Gli degradation in the absence of Sufu, have not been revealed.

Here we show that loss of *Spop* does not change the patterning of ventral spinal cord. This lack of spinal cord patterning defects does not result from redundancy with another Speckle-type POZ protein, Spop-like (Spopl), as the *Spopl;Spop* double mutant spinal cord is also properly patterned along its D/V axis. Interestingly, the level of Gli3 protein increases significantly in the *Spop* mutant spinal cords, and removing Spop rescues the loss of floor plate and V3 interneurons in *Gli2* mutants, suggesting that Spop negatively regulates Gli3A. On the other hand, no change in the level of Gli2 protein was observed in the absence of Spop, and the D/V patterning of *Spop;Gli3* double mutant spinal cord resembles that of *Gli3* mutants, suggesting that Gli2 is not the major target of Spop in the spinal cord. Furthermore, loss of *Spop* fails to restore the levels of Gli2 and Gli3 in *Sufu* mutants, but does exacerbate the ectopic activation of Shh signaling and ventralization of the spinal cord, and restores the formation of the floor plate and V3 interneurons in the *Gli1;Sufu* double mutant spinal cord. In summary, our data suggest that Spop negatively regulates Gli3A activity and Shh signaling, but does not underlie the drastic decrease in the levels of Gli2 and Gli3 in *Sufu* mutants.

2. Materials and Methods

2.1 Animal work

$Spop^{tm1a(KOMP)Mbp}$ ($Spop^{lacZKI}$) and $Spopl^{tm1(KOMP)Vlcg}$ were generated by Knockout Mouse Project (http://www.komp.org). The *Spop* loss-of-function allele used in the current study was generated by breeding $Spop^{lacZKI}$ mutant strain to *Tg(ACTFLPe)9205Dym/J* (Rodríguez et al., 2000) to remove the lacZ cassette flanked by FRT sites, and subsequently to *Tg(EIIa-Cre)C5379Lmgd/J* (Lakso et al., 1996) to delete exons 4 and 5. Other mouse strains used in this study were $Gli2^{tm2.1Alj}$ in which a *lacZ* inserted into exon 2 abolished *Gli2* expression (Bai and Joyner, 2001), $Gli3^{Xt\text{-}J}$ in which exons 10 to 15 were deleted resulting in a truncation following the first zinc finger motif (Hui and Joyner, 1993; Maynard et al., 2002), $Gli1^{tm2Alj}$ in which a *lacZ* cassette replaced exons 3 to 11 leading to expression of a non-functional *Gli1* mutant that lacked zinc finger domain at best (Bai et al., 2002), and $Sufu^{tm1Rto}$ in which a neomycin resistance cassette replaced exon 1 and prevented the expression of *Sufu* (Svard et al., 2006). All strains were kept on 129S2/SvPasCrl or C3H/HeNCrl (Charles River Lab) background and genotyped as previously described. The animal work in this study was approved by the IACUC at the Penn State University.

2.2 Quantitative real time polymerase chain reaction (qRT-PCR)

RNA was extracted with NucleoSpin RNA kit (Macherey-Nagel), and 1μg of RNA was used to synthesize cDNA with qScript cDNA Synthesis Kit (Quanta Biosciences, #95047-100). qRT-PCR was then performed in a StepOne Plus Real-time PCR system (Applied Biosystems) with PerfeCTa SYBR Green SuperMix (Quanta Biosciences). Primers used: Spopl, 5′-TCAACGTTTTCTTCAGGCCC-3′ and 5′-AAATCCCCAGTCCTTCCCCT-3′; Gapdh, 5′-GTCGGTGTGAACGGATTTGG-3′ and 5′-GACTCCACGACATACTCAGC-3′; Ptch1, 5′-CTCCAAGTGTCGTCCGGTTT-3′ and 5′-ACCCATTGTTCGTGTGACCA-3′; Gli1, 5′-CGTTTGAAGGCTGTCGGAAG-3′ and 5′-GCGTCTTGAGGTTTTCAAGGC-3′.

2.3 Immunoblot analysis

Embryos were homogenized in embryo lysis buffer (10mM Hepes/400mM NaCl/0.1mM EGTA/0.5mM DTT/10% glycerol/1% Triton X-100, pH 7.9) containing protease inhibitors. Protein concentration was measured with Pierce BCA Protein Assay kit (Thermo-Fisher) and equal amount of total proteins were loaded to each well. Nitrocellulose membranes were blocked with PBS/5% chicken serum and subject to primary antibody incubation in PBS/0.1% Tween-20/5% BSA, three washes in PBS/0.1% Tween-20, secondary antibody incubation in PBS/5% chicken serum and three washes in PBS/0.1% Tween-20. Primary antibodies used were Gli2 (R&D systems, AF3635, 1:500), Gli3 (R&D systems, AF3690, 1:200) and β-tubulin. Secondary antibodies were conjugated with fluorophores for detection with Odyssey Imaging Systems (LI-COR).

2.4 Immunohistochemistry

Embryos were lightly fixed with 4% paraformaldehyde (PFA) in PBS and cryosectioned at 10μm thickness. Sections were blocked in blocking buffer (PBS/1% goat serum/0.1% Triton X-100) and subject to primary antibody incubation, three washes, secondary antibody incubation and three washes. Antibody incubation and washes were all performed in blocking buffer. Primary antibodies used were Foxa2 (DSHB, 4C7, 1:40), Nkx2.2 (DSHB, 74.5A5, 1:40), Olig2 (Millipore, AB9610, 1:1000), Nkx6.1 (DSHB, F55A12, 1:500) and Pax6 (DSHB, 1:500). Secondary antibodies were Cy3-conjugated (Jackson Lab, 1:500). Slides were then mounted in DABCO (Sigma-Aldrich). Images were obtained with a Nikon E600 microscope and a QImaging Micropublisher Digital Camera.

3. Results

3.1 Loss of Spop leads to a moderate but significant increase in the level of Gli3 protein

To reveal the roles of Spop in Shh signaling and the D/V patterning of the spinal cord, we characterized two *Spop* loss-of-function mutant alleles. One mutant allele, $Spop^{lacZKI}$, contains a lacZ cassette knocked into the third intron of *Spop*, thus expresses lacZ under the control of *Spop* cis-regulatory elements (Fig. 1A). The other mutant allele, $Spop^{\Delta Ex}$, bears a deletion of the 4th and 5th exons of *Spop*, which was predicted to truncate the Spop protein at residue 26 due to a frame shift. Immunoblot analyses confirmed the absence of Spop protein in embryonic day (E) 10.5 homozygous mutant embryos for both alleles (Cai and

Liu, 2016). Both *Spop*^{lacZKI} and *Spop*$^{\Delta Ex}$ homozygous mutants exhibited neonatal lethality with skeletal defects (Cai and Liu, 2016). A small number of mutant embryos exhibited exencephaly (n= 11/157 homozygotes and 5/407 heterozygotes, combining both alleles) and spina bifida (n= 4/157 homozygotes, combining both alleles), suggesting that Spop may play a role in the development of the nervous system. For the rest of this study, we used *Spop*$^{\Delta Ex}$ exclusively to investigate the roles of *Spop* in spinal cord development, and will abbreviate it as *Spop* mutant or *Spop*$^{-}$.

Previous *in vitro* studies suggested that Spop targeted overexpressed Gli2 and Gli3 for degradation (Chen et al., 2009; Wang et al., 2010; Wen et al., 2010; Zhang et al., 2009). To investigate whether loss of *Spop* stabilizes Gli2 and Gli3 in the spinal cord, we examined the levels of these proteins in E10.5 embryos through immunoblotting analyses. We removed the heads, viscera and limbs from E10.5 embryos to specifically determine the protein levels in the spinal cord (Fig. 1E). Consistent with a role of Spop in Gli3 degradation, the levels of both full-length (Gli3FL) and repressor (Gli3R) forms of Gli3 were significantly increased in the *Spop* mutant spinal cord (Fig. 1G and H). In contrast, we did not observe an increase in the level of Gli2 in *Spop* mutants (Fig. 1F and H).

3.2 The D/V patterning of the Spop mutant spinal cord was normal

Most *Spop* mutant embryos resembled wild type morphologically (Fig. 2A, A′, G and G′). To investigate whether the increase in the level of Gli3 disrupted the D/V patterning of the spinal cord, we examined the expression of transcription factors specific for various groups of progenitor cells in the ventral spinal cord. At E9.5, *Foxa2* and *Nkx2.2* were both expressed in the ventral-most spinal cord (Fig. 2B and C), while at E10.5, *Foxa2* and *Nkx2.2* labeled the floor plate (FP) and progenitors of V3 interneurons (p3), respectively (Fig. 2H, I and M). *Olig2* labeled motor neuron progenitors (pMN) immediately dorsal to p3 (Fig. 2D, J and M). Nearly all ventral progenitor cells (p1, 2, 3 and pMN) expressed *Nkx6.1* (Fig. 2E, K and M). *Pax6* expression was present in dorsal and lateral regions of the spinal cord (Fig. 2F, L and M). We examined the expression patterns of these genes in both E9.5 and E10.5 *Spop* mutant spinal cords and found no change compared to their littermate controls (Fig. 2B′–F′ and H′–L′), suggesting that the moderate increase in the level of Gli3 was not sufficient to alter the early patterning of the ventral spinal cord. Consistent with this observation, the levels of *Ptch1* and *Gli1* expression were comparable between wild type and *Spop* mutant embryos, suggesting that Shh signaling activity was not affected by loss of *Spop* (Fig. S1A).

3.3 Loss of Spopl does not alter spinal cord patterning in wild type or Spop mutants

Spopl shares similar substrate specificity with Spop, albeit exhibiting weaker ubiquitin-ligase activity (Choo et al., 2010; Errington et al., 2012). To investigate whether Spopl functionally compensates for the loss of *Spop* in mouse development, especially the D/V patterning of the spinal cord, we acquired a *Spopl*$^{tm1(KOMP)Vlcg}$ mutant strain in which the entire coding region of *Spopl* was replaced with a *lacZ* reporter from KOMP (http://www.komp.org) (Fig. 1B). Since the entire coding region is deleted, *Spopl*$^{tm1(KOMP)Vlcg}$ (hereafter abbreviated as *Spopl*$^{-}$) is an absolute null mutant allele. By qRT-PCR, we found that *Spopl* was expressed in E9.5 mouse embryos, and its expression was reduced by half in *Spopl*$^{+/-}$ and undetectable in *Spopl*$^{-/-}$ embryos (Fig. 1C). *Spopl* homozygous mutants were

healthy and fertile (n >55 mutants weaned), and the E10.5 mutant spinal cords were patterned properly along the D/V axis, suggesting that Spopl did not play an essential role in mouse development and spinal cord D/V patterning (Fig. 3). Importantly, *Spopl;Spop* double mutant mice exhibit postnatal lethality, similar to *Spop* single mutants. We also found that the spinal cords were properly patterned in *Spopl;Spop* double mutants (Fig. 3). Furthermore, loss of *Spopl* did not affect the expression levels of *Ptch1* and *Gli1* (Fig. S1B). These data suggest that the Speckle-type POZ proteins, Spop and Spopl, are dispensable for the patterning of ventral spinal cord.

3.4 Loss of Spop restores normal patterning in the Gli2 mutant spinal cord

Neither Gli1 nor Gli3 was essential for the mammalian ventral spinal cord development (Bai et al., 2002; Park et al., 2000; Persson et al., 2002); however, the importance of these Gli proteins in supporting maximal Shh signaling and ventral spinal cord development was revealed with simultaneous reduction or ablation of Gli2, suggesting that these three Gli proteins share redundant functions in spinal cord patterning (Bai et al., 2004; Lei et al., 2004; Park et al., 2000). This functional redundancy among the three mouse Gli proteins suggests that a moderate change in the activities of any member of this family may have a more obvious impact in the spinal cord pattering in the absence of another Gli protein. We hence removed *Gli2* in *Spop* mutants to determine whether the increase in the level of Gli3 rescues the spinal cord patterning defects resulting from loss of *Gli2*. The morphology of *Spop;Gli2* double mutant embryos resembled that of *Gli2* mutants at E10.5 (Fig. 4A–A″). As reported previously (Ding et al., 1998; Matise et al., 1998), the *Foxa2*-expressing FP was missing and *Nkx2.2*-expressing p3 cells were diminished in the *Gli2* mutant spinal cord (Fig. 4B′, C′), whereas *Olig2* expression was expanded to the ventral midline (Fig. 4D′). Interestingly, *Foxa2* was expressed, and *Nkx2.2* expression was increased, in the *Spop;Gli2* double mutant spinal cord (Fig. 4B″ and C″). Meanwhile, *Olig2* expression was excluded from the ventral-most part of the *Spop;Gli2* double mutant spinal cord (Fig. 4D″). The *Nkx6.1* expression domain, which includes cell types that do not require high levels of Shh pathway activation, and *Pax6* expression domain, which includes cell types that are inhibited by high levels of Shh activation, were similar in wild type, *Gli2* mutants and *Spop;Gli2* double mutants (Fig. 4E–F″). We observed similar restoration of the spinal cord patterning in E9.5 *Spop;Gli2* double mutants (Fig. S2). The restored formation of FP and p3 in the *Spop;Gli2* double mutant spinal cords suggested an increase in Shh pathway activation. Supporting this hypothesis, the expression levels of *Ptch1* and *Gli1* were decreased in *Gli2* mutant embryos, and restored in *Spop;Gli2* double mutants (Fig. S1C), suggesting that loss of *Spop* enhanced Shh signaling activity, which underlies the rescue of spinal cord patterning defect caused by loss of *Gli2*. Theoretically, changes in the activities of both Gli1 and Gli3 could contribute to this increase; however, previous in vitro studies suggested that Spop did not target Gli1 for degradation (Chen et al., 2009; Zhang et al., 2009). Therefore, the increase in the activation of the Shh pathway in *Spop;Gli2* double mutants likely results from an increase in the Gli3A activity (Fig. 1G), which is better revealed in the absence of Gli2.

3.5 The ventral spinal cord was properly patterned in Spop;Gli3 double mutants

In contrast to the moderate increase in the level of Gli3, the level of Gli2 was not changed in *Spop* mutant neural tube (Fig. 1F and H). However, we could not rule out the possibility that Spop might regulate Gli2 activity without affecting its protein level. As the presence of Gli3 repressor in the spinal cord may conceal the effect of any moderate increase in Gli2 activator activity, we sought to reveal such increase by removing *Gli3* in *Spop* mutants. As previously reported, loss of *Gli3* led to frequent exencephaly at E10.5 (Fig. 5A and A′), but had no impact on the expression of *Foxa2, Nkx2.2, Olig2, Nkx6.1* and *Pax6* (Fig. 5B–F′). If loss of *Spop* increased Gli2 activity, a dorsal expansion of *FoxA2*, *Nkx2.2*, *Olig2* or *Nkx6.1* expression would be expected in *Spop;Gli3* double mutants. In contrast, *Spop;Gli3* double mutant embryos resembled *Gli3* mutants morphologically (Fig. 5A″), and did not exhibit any change in the expression patterns of these genes in the ventral spinal cord (Fig. 5B″–F″). Similarly, *Spop;Gli3* double mutants resembled *Gli3* mutants both in morphology and in spinal cord patterning at E9.5 (Fig. S3). These data suggest that loss of *Spop* does not result in a noticeable increase in Gli2 activity, consistent with the unchanged Gli2 level in *Spop* mutants (Fig. 1F, H).

3.6 Loss of Spop exacerbates the spinal cord patterning defects in Sufu mutants

A well-known negative regulator of Shh signaling, Sufu, is expressed in the spinal cord and plays an essential role in spinal cord D/V patterning (Cooper et al., 2005; Stone et al., 1999; Svard et al., 2006). We and others have previously shown that the levels of Gli2 and Gli3 were drastically reduced in *Sufu* mutants, suggesting that in addition to its inhibitory function, Sufu may also protect Gli2 and Gli3 from degradation (Chen et al., 2009; Jia et al., 2009; Wang et al., 2010). It was suggested that Spop might underlie the degradation of Gli2 and Gli3 in the absence of Sufu, and prevent the full activation of Hh pathway (Chen et al., 2009; Wang et al., 2010). To test this hypothesis, we performed immunoblot analyses on E9.5 *Spop;Sufu* double mutant embryos. We found a moderate increase in the level of Gli3FL in *Spop;Sufu* double mutants than in *Sufu* single mutants, although the difference did not reach statistical significance (Fig. 6). In contrast, the levels of Gli2 and Gli3R were comparable between *Spop;Sufu* double mutants and *Sufu* single mutants. Nevertheless, the levels of both Gli2 and Gli3 in *Spop;Sufu* double mutants were still significantly lower than those in wild type littermates, suggesting that *Spop* was not solely accountable for the drastic reduction of Gli2 and Gli3 in *Sufu* mutants (Fig. 6).

We next sought to investigate whether the moderate increase in the level of Gli3FL had an impact on the morphology and spinal cord patterning of *Spop;Sufu* double mutants. Consistent with our previous report (Liu et al., 2012), E9.5 *Sufu* mutant embryos exhibited twisted body axis and severe neural tube closure defects (Fig. 7A′). The *Sufu* mutant spinal cord was severely ventralized, with strong *Foxa2, Nkx2.2* and *Nkx6.1* expression throughout the D/V axis (Fig. 7B′–D′). *Olig2* expression was strong in the dorsal spinal cord, but appeared weaker and scattered ventrally, consistent with its being activated by low levels of Shh signaling but repressed by high levels of Shh signaling (Fig. 7E′). Consistent with the hyperactivation of Shh signaling, *Pax6* expression was restricted to just a few cells in the dorsal spinal cord of *Sufu* mutants (Fig. 7F′). *Spop;Sufu* double mutant embryos failed to turn, and exhibited severe neural tube closure defects like *Sufu* single mutants (Fig. 7A″).

Similar to *Sufu* mutants, the *Spop;Sufu* double mutant spinal cord exhibited widespread expression of *Foxa2, Nkx2.2* and *Nkx6.1* (Fig. 7B″–D″). Furthermore, *Olig2* expression was only found in a few dorsal cells (Fig. 7E″), and *Pax6* expression was completely absent, in the *Spop;Sufu* double mutant spinal cord (Fig. 7F″). These data indicate that loss of *Spop* leads to more severe ventralization of the spinal cords in the absence of Sufu.

Although it is formally possible that Spop may regulate an unknown process that indirectly affects the D/V patterning of the spinal cord, the similarity between the morphological and patterning defects between *Spop;Sufu* double mutants and those of previously reported *Ptch1* mutants (Goodrich et al., 1997) and *Sufu;Gli3* double mutants (Liu et al., 2012) suggests that the extreme ventralization of the spinal cord was likely the direct result of the hyperactivation of the Shh pathway due to loss of both *Spop* and *Sufu*.

3.7 Loss of Spop restored the ventral-most cell fates in the Gli1; Sufu double mutant spinal cord

We previously found that the FP and p3, the ventral-most cell types in the spinal cord, were lost in *Gli1;Sufu* double mutants, but not in *Gli1* single mutants, indicating a positive role of Sufu in Hh pathway activation (Liu et al., 2012). We hypothesized that Spop-mediated degradation of activated Gli2 and/or Gli3 in the absence of *Sufu* might underlie the loss of ventral cell types in *Gli1;Sufu* double mutants. Although the above immunoblot analyses (see Fig. 6) suggested that loss of *Spop* could not fully restore the levels of Gli2 and Gli3, we were encouraged by the exacerbation of the *Sufu* mutant spinal cord defects resulting from the additional loss of *Spop*, and tested the impact of loss of *Spop* on the spinal cord patterning defects of *Gli1;Sufu* double mutants. E9.5 *Gli1;Sufu* double mutant embryos exhibited less severe neural tube closure defects than *Sufu* single mutants, especially in the anterior part of the embryos (compare Fig. 8A′ to Fig. 7A′). Consistent with our previous report (Liu et al., 2012), fewer *Foxa2*- and *Nkx2.2*-expressing cells were present in the E9.5 *Gli1;Sufu* double mutant spinal cord compared to *Gli1* single mutants (Fig. 8B–C′). Meanwhile, the *Olig2* and *Pax6* expression domains were expanded toward the ventral midline (Fig. 8D, D′, F and F′), suggesting that *Sufu* was required for the full activation of Hh pathway in the absence of *Gli1*. The *Olig2* and *Nkx6.1* domains were also expanded more dorsally in *Gli1;Sufu* double mutants than in *Gli1* single mutants, suggesting that lower levels of ectopic activation of Shh signaling persisted in the double mutants (Fig. 8D–E′). In contrast, *Spop;Gli1;Sufu* triple mutants exhibited widespread edema in addition to more severe neural tube closure defects than those of *Gli1;Sufu* double mutants (Fig. 8A″). Interestingly, the expression domains of *Foxa2, Nkx2.2* and *Nkx6.1* were all dorsally expanded in *Spop;Gli1;Sufu* triple mutants, indicating higher levels of Shh pathway activation in the absence of *Spop* (Fig. 8B″, C″ and E″). Moreover, the expression of *Olig2* and *Pax6*, which was inhibited by high levels of Shh signaling, was restricted to the dorsal regions of the spinal cord in *Spop;Gli1;Sufu* triple mutants (Fig. 8D″ and F″). These results suggest that Spop plays a negative role in Shh pathway activation and ventral spinal cord development, and accounts for the lack of maximal activation of Shh pathway in *Gli1;Sufu* double mutant embryos.

To assess the Shh pathway activity more directly, we examined the expression of the lacZ reporter inserted into the *Gli1* locus (*Gli1-lacZ*). As reported previously, *Gli1-lacZ* expression formed a ventral-to-dorsal gradient in the *Gli1* mutant spinal cord, consistent with the existence of a ventral-to-dorsal Shh signaling gradient (Fig. 8G; Bai et al., 2002). A notable exception was the floor plate, in which prolonged exposure to extremely high Shh activity resulted in a downregulation of *Gli1-lacZ* expression, as previously reported (Fig. 8G; Ribes et al., 2010). Consistent with the widespread low and intermediate levels of Shh pathway activation but lack of maximal Shh pathway activation, strong *Gli1-lacZ* expression is present throughout the entire *Gli1;Sufu* double mutant spinal cord (Fig. 8G′). Interestingly, *Gli1-lacZ* is downregulated in the ventral region of the *Spop;Gli1;Sufu* triple mutant spinal cords, suggesting the restoration of maximal activation of Shh signaling (Fig. 8G″). Combined with the above spinal cord D/V patterning analyses, we conclude that loss of *Spop* allows maximal activation of Shh pathway in the absence of *Gli1* and *Sufu*.

4. Discussion

Despite extensive studies in *Drosophila* and cultured cells (Chen et al., 2009; Kent et al., 2006; Seong et al., 2010; Wang et al., 2010; Wen et al., 2010; Zhang et al., 2009; Zhang et al., 2006), the *in vivo* function of Spop in Shh signaling and mouse spinal cord ventral patterning has not been revealed. In the present study, we show that Spop negatively regulates the protein level of Gli3, but not Gli2. As a result, ventral spinal cord patterning in *Gli2* mutants, in which Gli3 activator acts as the primary effector of the Shh pathway, is subject to Spop regulation. In addition, we reveal a role of Spop in dampening Shh pathway over-activation in the absence of *Sufu*, especially in preventing the maximal activation of Shh signaling and the ventral-most cell fates in the *Gli1;Sufu* double mutant spinal cord (Fig. 9).

In *Drosophila*, the loss of *roadkill (hib/rdx)*, the homolog of Spop, results in an obvious activation of Hh signaling, which is in striking contrast to the normal Shh-dependent D/V patterning of the spinal cord in *Spop* null mutants (Kent et al., 2006; Seong et al., 2010; Zhang et al., 2006). Two factors may underlie this difference. First, the *Drosophila hib/rdx* is highly expressed only in cells experiencing high levels of Hh pathway activation, whereas mouse *Spop* is expressed at low levels throughout the spinal cord. Second, cubitus interruptus (ci) is the only Gli family member in *Drosophila* and it is targeted by hib/rdx for degradation. In contrast, there are three mammalian Gli family members, and Gli3, better known for its repressor function in Hh signaling, appears to be the only endogenous target for Spop-mediated degradation. Therefore, it is not surprising that loss of *Spop* only impacts the spinal cord patterning in the absence of Gli2.

Previous studies showed that Spop targets both Gli2 and Gli3 for degradation *in vitro* (Chen et al., 2009; Wang et al., 2010; Wen et al., 2010; Zhang et al., 2009; Zhang et al., 2006). In contrast, the level of Gli3, but not Gli2, increased in *Spop* mutant embryos. Since Spop interacts with both the N and C termini of Gli3 but only with the C terminus of Gli2, it is possible that Spop preferentially binds Gli3 but not Gli2 under physiological condition (Wang et al., 2010; Zhang et al., 2009). Alternatively, Gli2 may be associated with other

proteins that prevent its interaction with Spop, or protect it from subsequent degradation *in vivo*.

Previous *in vitro* studies showed that RNAi knockdown of Spop restored the levels of Gli2 and Gli3 to, or even above the wild type level in *Sufu* mutant cells (Chen et al., 2009; Wang et al., 2010) or cells treated with Shh (Wen et al., 2010). In contrast, our data show that removal of *Spop* has no impact on the level of Gli2 and only moderately increases the level of Gli3FL in *Sufu* mutant embryos (Fig. 6). The difference between our observation and the previous ones could reflect the intrinsic difference between the permanent knockout mutant embryos and cells in culture with transient knockdown of the Spop protein. Recent studies have shown that compensatory mechanisms might be activated only in mutant embryos, but not in transient knockdown assays (e.g. Hall et al., 2013). It will be interesting to investigate whether this is indeed the case in *Spop* mutants.

Despite the lack of full restoration of the levels of Gli2 and Gli3 (Fig. 6), we show that removing Spop does result in more extreme ventralization of the *Sufu* mutant spinal cord and rescue the formation of the FP and p3 interneuron progenitors in the *Gli1;Sufu* double mutant spinal cord, suggesting higher levels of Shh signaling in both cases. It is possible that the moderate increase in Gli3FL is sufficient for this increase in Hh pathway activity in the absence of Spop. Alternatively, Spop may inhibit Gli activator activities through additional, degradation-independent mechanisms. Interestingly, a recent work showed that hib/rdx inhibits the maximal activation of Hh signaling at the border between the anterior and posterior compartments of the wing disc by sequestering ci in the cytoplasm (Seong et al., 2010). It is possible that a similar mechanism may partially underlie Spop function in mammals as overexpression of *Spop* appears to sequester Gli3 in the cytoplasm in cultured cells (Chen et al., 2009 and data not shown). An antibody that specifically recognizes Gli3FL will allow us to investigate whether this is true with endogenous Gli3.

Due to difficulty in breeding *Spop;Sufu* double mutants, we analyzed spinal cord patterning in only two *Spop;Sufu* double mutant embryos. However, these two double mutants both exhibited more extreme ventralization of the spinal cord than *Sufu* mutants. Importantly, the comparison between *Gli1;Sufu* double and *Spop;Gli1;Sufu* triple mutants also show the exacerbation of spinal cord ventralization and Shh signaling activation as the result of loss of *Spop.* Therefore, we are confident at the conclusion that *Spop* plays an important negative role in Shh pathway activation in the absence of *Sufu*.

Spopl shares similar substrate specificity as Spop, but exhibits much weaker ubiquitin-ligase activity *in vitro* (Errington et al., 2012). It was suggested that Spopl interferes with the more efficient Spop and may have a dominant-negative effect. However, we did not observe any morphological or patterning defects in *Spopl* mutants, and *Spopl;Spop* double mutants appear to be identical to *Spop* mutants. These suggest that functional redundancy between these two speckle-type POZ proteins does not underlie the lack of noticeable patterning defects in the *Spop* mutant spinal cord.

In recent years, it has become increasingly appreciated that prolonged exposure to Shh ligand changes the sensitivity of the spinal cord cells to the ligand, a phenomenon termed as

adaptation (Balaskas et al., 2012; Dessaud et al., 2010; Ribes et al., 2010). A mathematical model has been proposed that involves transcriptional upregulation of *Ptch1*, transcriptional downregulation of the *Gli* genes, and differential degradation of the Gli activators as important contributing factors for adaptation (Cohen et al, 2015). As previous *in vitro* studies suggested that Spop differentially targets the activator form of Gli3 for degradation, the increase in Hh pathway activation in E9.5 *Spop;Gli2* double mutants as indicated by the levels of *Ptch1* and *Gli1* transcription could result, at least partly, from altered adaptation (see Fig. S1C). A closer scrutiny at the temporal profile of Shh pathway activity in this mutant will help to provide a more definitive answer.

In conclusion, we find an *in vivo* role of Spop in Gli3 degradation and ventral spinal cord patterning better revealed in the absence of *Gli2*. Loss of *Spop* in the absence of *Sufu* exacerbates Hh pathway over-activation and spinal cord ventralization without fully restoring the levels of Gli2 and Gli3 proteins. Our results provide insight into the roles of Spop in the regulation of Gli3 activity and spinal cord development *in vivo,* and suggest more complexity in the mechanisms of Spop function unappreciated in previous *in vitro* studies. They also raise new questions such as what, if not Spop, is responsible for the drastic reduction of Gli2 and Gli3 in *Sufu* mutants, which will continue to be an interesting question awaiting an answer.

Supplementary Material

Refer to Web version on PubMed Central for supplementary material.

Acknowledgments

We thank Drs Zhi-Chun Lai and Wendy Hanna-Rose for critically reading the manuscript. We thank Drs Joyner and Toftgard for *Gli1, Gli2, Gli3* and *Sufu* mutant mice. The monoclonal antibodies against Foxa2, Nkx2.2, Nkx6.1 and Pax6 developed by Drs. Jessell, Madsen and Kawakami were obtained from the Developmental Studies Hybridoma Bank developed under the auspices of the NICHD and maintained by The University of Iowa, Department of Biological Sciences, Iowa City, IA 52242. A.L. was supported by the National Institutes of Health [grant number HD083625] and a Penn State Start-up Fund.

References

Bai CB, Auerbach W, Lee JS, Stephen D, Joyner AL. Gli2, but not Gli1, is required for initial Shh signaling and ectopic activation of the Shh pathway. Development. 2002; 129:4753–61. [PubMed: 12361967]

Bai CB, Joyner AL. Gli1 can rescue the in vivo function of Gli2. Development. 2001; 128:5161–72. [PubMed: 11748151]

Bai CB, Stephen D, Joyner AL. All mouse ventral spinal cord patterning by hedgehog is Gli dependent and involves an activator function of Gli3. Dev Cell. 2004; 6:103–15. [PubMed: 14723851]

Balaskas N, Ribeiro A, Panovska J, Dessaud E, Sasai N, Page KM, Briscoe J, Ribes V. Gene regulatory logic for reading the Sonic Hedgehog signaling gradient in the vertebrate neural tube. Cell. 2012; 148:273–84. [PubMed: 22265416]

Barnfield PC, Zhang X, Thanabalasingham V, Yoshida M, Hui CC. Negative regulation of Gli1 and Gli2 activator function by Suppressor of fused through multiple mechanisms. Differentiation. 2005; 73:397–405. [PubMed: 16316410]

Briscoe J, Therond PP. The mechanisms of Hedgehog signalling and its roles in development and disease. Nat Rev Mol Cell Biol. 2013; 14:416–29. [PubMed: 23719536]

Cai H, Liu A. Spop promotes skeletal development and homeostasis by positively regulating Ihh signaling. Proc Natl Acad Sci U S A. 2016; 113:14751–14756. [PubMed: 27930311]

Chen MH, Wilson CW, Li YJ, Law KK, Lu CS, Gacayan R, Zhang X, Hui CC, Chuang PT. Cilium-independent regulation of Gli protein function by Sufu in Hedgehog signaling is evolutionarily conserved. Genes Dev. 2009; 23:1910–28. [PubMed: 19684112]

Cheng SY, Bishop JM. Suppressor of Fused represses Gli-mediated transcription by recruiting the SAP18-mSin3 corepressor complex. Proc Natl Acad Sci U S A. 2002; 99:5442–7. [PubMed: 11960000]

Choo KB, Chuang TJ, Lin WY, Chang CM, Tsai YH, Huang CJ. Evolutionary expansion of SPOP and associated TD/POZ gene family: impact of evolutionary route on gene expression pattern. Gene. 2010; 460:39–47. [PubMed: 20399258]

Cohen M, Briscoe J, Blassberg R. Morphogen interpretation: the transcriptional logic of neural tube patterning. Curr Opin Genet Dev. 2013; 23:423–8. [PubMed: 23725799]

Cooper AF, Yu KP, Brueckner M, Brailey LL, Johnson L, McGrath JM, Bale AE. Cardiac and CNS defects in a mouse with targeted disruption of suppressor of fused. Development. 2005; 132:4407–17. [PubMed: 16155214]

Dessaud E, Ribes V, Balaskas N, Yang LL, Pierani A, Kicheva A, Novitch BG, Briscoe J, Sasai N. Dynamic assignment and maintenance of positional identity in the ventral neural tube by the morphogen sonic hedgehog. PLoS Biol. 2010; 8:e1000382. [PubMed: 20532235]

Ding Q, Fukami S, Meng X, Nishizaki Y, Zhang X, Sasaki H, Dlugosz A, Nakafuku M, Hui C. Mouse suppressor of fused is a negative regulator of sonic hedgehog signaling and alters the subcellular distribution of Gli1. Curr Biol. 1999; 9:1119–22. [PubMed: 10531011]

Ding Q, Motoyama J, Gasca S, Mo R, Sasaki H, Rossant J, Hui CC. Diminished Sonic hedgehog signaling and lack of floor plate differentiation in Gli2 mutant mice. Development. 1998; 125:2533–43. [PubMed: 9636069]

Dunaeva M, Michelson P, Kogerman P, Toftgard R. Characterization of the physical interaction of Gli proteins with SUFU proteins. J Biol Chem. 2003; 278:5116–22. [PubMed: 12426310]

Errington WJ, Khan MQ, Bueler SA, Rubinstein JL, Chakrabartty A, Prive GG. Adaptor protein self-assembly drives the control of a cullin-RING ubiquitin ligase. Structure. 2012; 20:1141–53. [PubMed: 22632832]

Goodrich LV, Milenkovic L, Higgins KM, Scott MP. Altered neural cell fates and medulloblastoma in mouse patched mutants. Science. 1997; 277:1109–13. [PubMed: 9262482]

Hall EA, Keighren M, Ford MJ, Davey T, Jarman AP, Smith LB, Jackson IJ, Mill P. Acute versus chronic loss of mammalian Azi1/Cep131 results in distinct ciliary phenotypes. PLoS Genet. 2013; 9:e1003928. [PubMed: 24415959]

Hui CC, Joyner AL. A mouse model of greig cephalopolysyndactyly syndrome: the extra-toesJ mutation contains an intragenic deletion of the Gli3 gene PG - 241–6. Nat Genet. 1993; 3

Humke EW, Dorn KV, Milenkovic L, Scott MP, Rohatgi R. The output of Hedgehog signaling is controlled by the dynamic association between Suppressor of Fused and the Gli proteins. Genes Dev. 2010; 24:670–82. [PubMed: 20360384]

Jia J, Kolterud A, Zeng H, Hoover A, Teglund S, Toftgard R, Liu A. Suppressor of Fused inhibits mammalian Hedgehog signaling in the absence of cilia. Dev Biol. 2009; 330:452–60. [PubMed: 19371734]

Kent D, Bush EW, Hooper JE. Roadkill attenuates Hedgehog responses through degradation of Cubitus interruptus. Development. 2006; 133:2001–10. [PubMed: 16651542]

Kogerman P, Grimm T, Kogerman L, Krause D, Unden AB, Sandstedt B, Toftgard R, Zaphiropoulos PG. Mammalian suppressor-of-fused modulates nuclear-cytoplasmic shuttling of Gli-1. Nat Cell Biol. 1999; 1:312–9. [PubMed: 10559945]

Lakso M, Pichel JG, Gorman JR, Sauer B, Okamoto Y, Lee E, Alt FW, Westphal H. Efficient in vivo manipulation of mouse genomic sequences at the zygote stage. Proc Natl Acad Sci U S A. 1996; 93:5860–5. [PubMed: 8650183]

Lei Q, Zelman AK, Kuang E, Li S, Matise MP. Transduction of graded Hedgehog signaling by a combination of Gli2 and Gli3 activator functions in the developing spinal cord. Development. 2004; 131:3593–604. [PubMed: 15215207]

Lin C, Yao E, Wang K, Nozawa Y, Shimizu H, Johnson JR, Chen JN, Krogan NJ, Chuang PT. Regulation of Sufu activity by p66beta and Mycbp provides new insight into vertebrate Hedgehog signaling. Genes Dev. 2014; 28:2547–63. [PubMed: 25403183]

Liu J, Heydeck W, Zeng H, Liu A. Dual function of suppressor of fused in Hh pathway activation and mouse spinal cord patterning. Dev Biol. 2012; 362:141–53. [PubMed: 22182519]

Matise MP, Epstein DJ, Park HL, Platt KA, Joyner AL. Gli2 is required for induction of floor plate and adjacent cells, but not most ventral neurons in the mouse central nervous system PG - 2759–70. Development. 1998:125. [PubMed: 9389670]

Matise MP, Joyner AL. Gli genes in development and cancer. Oncogene. 1999; 18:7852–9. [PubMed: 10630638]

Maynard TM, Jain MD, Balmer CW, LaMantia AS. High-resolution mapping of the Gli3 mutation extra-toes reveals a 51.5-kb deletion. Mamm Genome. 2002; 13:58–61. [PubMed: 11773971]

Merchant M, Vajdos FF, Ultsch M, Maun HR, Wendt U, Cannon J, Desmarais W, Lazarus RA, de Vos AM, de Sauvage FJ. Suppressor of fused regulates Gli activity through a dual binding mechanism. Mol Cell Biol. 2004; 24:8627–41. [PubMed: 15367681]

Murone M, Luoh SM, Stone D, Li W, Gurney A, Armanini M, Grey C, Rosenthal A, de Sauvage FJ. Gli regulation by the opposing activities of fused and suppressor of fused. Nat Cell Biol. 2000; 2:310–2. [PubMed: 10806483]

Paces-Fessy M, Boucher D, Petit E, Paute-Briand S, Blanchet-Tournier MF. The negative regulator of Gli, Suppressor of fused (Sufu), interacts with SAP18, Galectin3 and other nuclear proteins. Biochem J. 2004; 378:353–62. [PubMed: 14611647]

Pan Y, Bai CB, Joyner AL, Wang B. Sonic hedgehog signaling regulates Gli2 transcriptional activity by suppressing its processing and degradation. Mol Cell Biol. 2006; 26:3365–77. [PubMed: 16611981]

Park HL, Bai C, Platt KA, Matise MP, Beeghly A, Hui CC, Nakashima M, Joyner AL. Mouse Gli1 mutants are viable but have defects in SHH signaling in combination with a Gli2 mutation PG - 1593–605. Development. 2000:127.

Persson M, Stamataki D, te Welscher P, Andersson E, Bose J, Ruther U, Ericson J, Briscoe J. Dorsal-ventral patterning of the spinal cord requires Gli3 transcriptional repressor activity. Genes Dev. 2002; 16:2865–78. [PubMed: 12435629]

Ribes V, Balaskas N, Sasai N, Cruz C, Dessaud E, Cayuso J, Tozer S, Yang LL, Novitch B, Marti E, Briscoe J. Distinct Sonic Hedgehog signaling dynamics specify floor plate and ventral neuronal progenitors in the vertebrate neural tube. Genes Dev. 2010; 24:1186–200. [PubMed: 20516201]

Rodríguez CI, Buchholz F, Galloway J, Sequerra R, Kasper J, Ayala R, Stewart AF, Dymecki SM. High-efficiency deleter mice show that FLPe is an alternative to Cre-loxP. Nat Genet. 2000; 25:139–40. [PubMed: 10835623]

Seong KH, Akimaru H, Dai P, Nomura T, Okada M, Ishii S. Inhibition of the nuclear import of cubitus interruptus by roadkill in the presence of strong hedgehog signal. PLoS One. 2010; 5:e15365. [PubMed: 21179535]

Stone DM, Murone M, Luoh S, Ye W, Armanini MP, Gurney A, Phillips H, Brush J, Goddard A, de Sauvage FJ, Rosenthal A. Characterization of the human suppressor of fused, a negative regulator of the zinc-finger transcription factor Gli. J Cell Sci. 1999; 112(Pt 23):4437–48. [PubMed: 10564661]

Svard J, Heby-Henricson K, Persson-Lek M, Rozell B, Lauth M, Bergstrom A, Ericson J, Toftgard R, Teglund S. Genetic elimination of Suppressor of fused reveals an essential repressor function in the mammalian Hedgehog signaling pathway. Dev Cell. 2006; 10:187–97. [PubMed: 16459298]

Theil T, Alvarez-Bolado G, Walter A, Ruther U. Gli3 is required for Emx gene expression during dorsal telencephalon development. Development. 1999; 126:3561–71. [PubMed: 10409502]

Tole S, Ragsdale CW, Grove EA. Dorsoventral patterning of the telencephalon is disrupted in the mouse mutant extra-toes(J). Dev Biol. 2000; 217:254–65. [PubMed: 10625551]

Tukachinsky H, Lopez LV, Salic A. A mechanism for vertebrate Hedgehog signaling: recruitment to cilia and dissociation of SuFu-Gli protein complexes. J Cell Biol. 2010; 191:415–28. [PubMed: 20956384]

Wang B, Fallon JF, Beachy PA. Hedgehog-regulated processing of Gli3 produces an anterior/posterior repressor gradient in the developing vertebrate limb. Cell. 2000; 100:423–34. [PubMed: 10693759]

Wang C, Pan Y, Wang B. Suppressor of fused and Spop regulate the stability, processing and function of Gli2 and Gli3 full-length activators but not their repressors. Development. 2010; 137:2001–9. [PubMed: 20463034]

Wen X, Lai CK, Evangelista M, Hongo JA, de Sauvage FJ, Scales SJ. Kinetics of hedgehog-dependent full-length Gli3 accumulation in primary cilia and subsequent degradation. Mol Cell Biol. 2010; 30:1910–22. [PubMed: 20154143]

Zhang Q, Shi Q, Chen Y, Yue T, Li S, Wang B, Jiang J. Multiple Ser/Thr-rich degrons mediate the degradation of Ci/Gli by the Cul3-HIB/SPOP E3 ubiquitin ligase. Proc Natl Acad Sci U S A. 2009; 106:21191–6. [PubMed: 19955409]

Zhang Q, Zhang L, Wang B, Ou CY, Chien CT, Jiang J. A hedgehog-induced BTB protein modulates hedgehog signaling by degrading Ci/Gli transcription factor. Dev Cell. 2006; 10:719–29. [PubMed: 16740475]

Highlights

- Spop and Spop-like are dispensable for the dorsoventral patterning of the mouse spinal cord.
- Loss of Spop leads to a significant increase in the level of Gli3, but not Gli2, in the mouse spinal cord.
- Removing *Spop* rescues the formation of the floor plate and V3 interneuron progenitors, cell types requiring the maximal activation of Shh signaling, in the absence of Gli2, consistent with an increase in Gli3 activator activity.
- Removing *Spop* allows more extreme Hh pathway activation and spinal cord ventralization in the absence of *Sufu*, and restores the formation of the floor plate and V3 interneuron progenitors in the absence of *Sufu* and *Gli1*.
- Loss of *Spop* results in a moderate increase in the level of Gli3 in the absence of *Sufu*, but fails to restore the level of Gli2 or Gli3 to the wild type level, suggesting additional mechanisms underlying Gli protein level regulation in *Sufu* mutants.

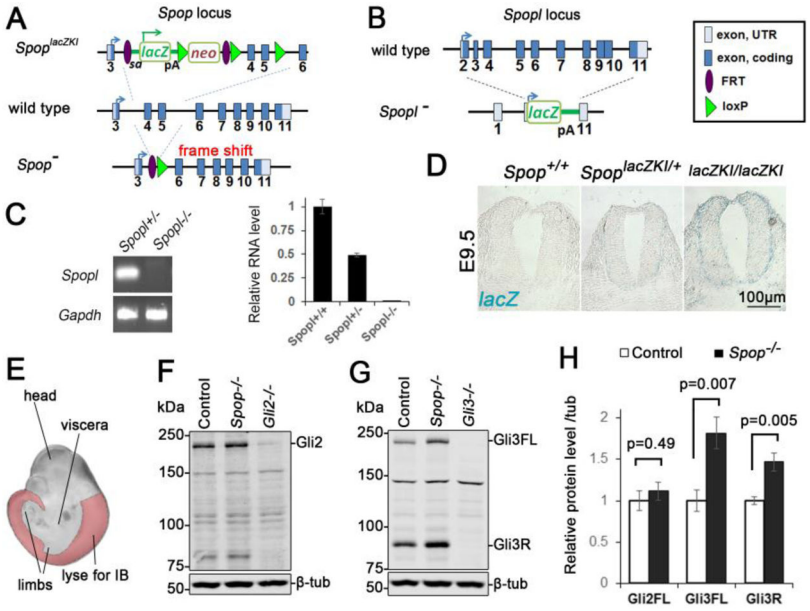

Fig. 1. A moderate increase in Gli3 protein level in the *Spop* mutant spinal cords

(A) A schematic illustration of *Spop* loss-of-function mutant alleles. $Spop^{lacZKI}$ contained a lacZ and neomycin resistance cassette. $Spop^{\Delta Ex}$ was generated from recombination of introduced FRT and loxP sites that deletes the 4th and 5th exons. This deletion also resulted in a frame shift that truncated the protein. (B) A schematic illustration of *Spopl* null mutant allele, in which a *lacZ* reporter replaced the entire protein-coding region of *Spopl*. pA: polyA signal. (C) Quantitative real time PCR showing the absence of *Spopl* transcript in E9.5 *Spopl* mutant embryos (mean ± SEM, n=3 wild type, 4 $Spopl^{+/-}$ and 5 $Spopl^{-/-}$ embryos). (D) X-gal staining of E9.5 $Spop^{lacZKI}$ heterozygotes and homozygotes showing *Spop* expression in the neural tube. (E) A schematic illustration of tissue (highlighted region) used for immunoblot in (F) and (G). The trunks of E10.5 embryos were freed of viscera and limbs to minimize the effect of Gli proteins in these tissues. (F) Immunoblots with antibodies against Gli2 and β-tubulin. (G) Immunoblots with antibodies against Gli3 and β-tubulin. (H) Quantification of (F) and (G) (mean ± SEM from n=6 embryos per group). Student's *t*-test showed a significant increase in the levels of Gli3FL and Gli3R, but not Gli2 in *Spop* mutants.

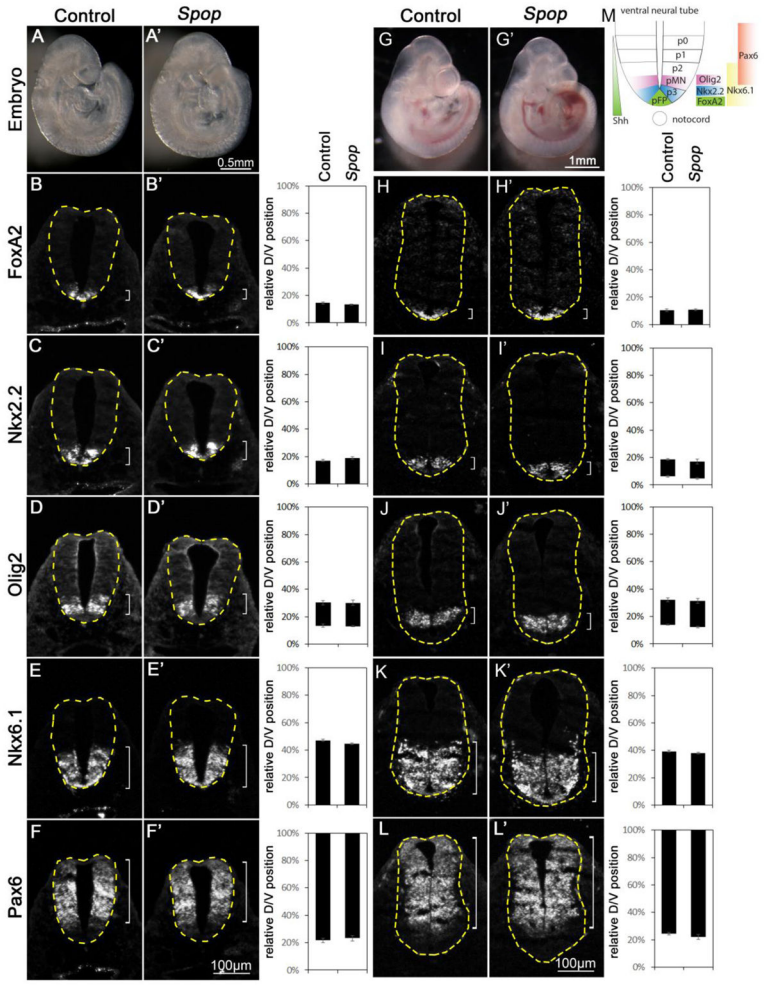

Fig. 2. Normal ventral patterning of the *Spop* mutant spinal cords

(A, A′) Lateral views of E9.5 control (A) and *Spop* (A′) mutant embryos. (B–F′) Immunofluorescent images of transverse sections of E9.5 control (n=4 embryos) and *Spop* mutant (n=4 embryos) spinal cords at the forelimb level with indicated antibodies. (G, G′) Lateral views of E10.5 control (G) and *Spop* (G′) mutant embryos. (H–L′) Immunofluorescent images of transverse sections of E10.5 control (n=4 embryos) and *Spop* mutant (n=4 embryos) spinal cords at the forelimb level. The spinal cords are outlined with dash lines. Brackets indicate the expression domains. The span of each domain along the D/V axis is quantified and shown on the right. Relative D/V position is shown as the distance to the ventral-most point of the spinal cord as a percentage of the entire D/V span of the spinal cord. Student's *t*-test suggests no significant difference between *Spop* mutant and control groups. (M) A schematic illustration of ventral spinal cord patterning at E10.5 depicting the arrangement of various progenitor groups and the expression domains of marker genes in wild type embryos.

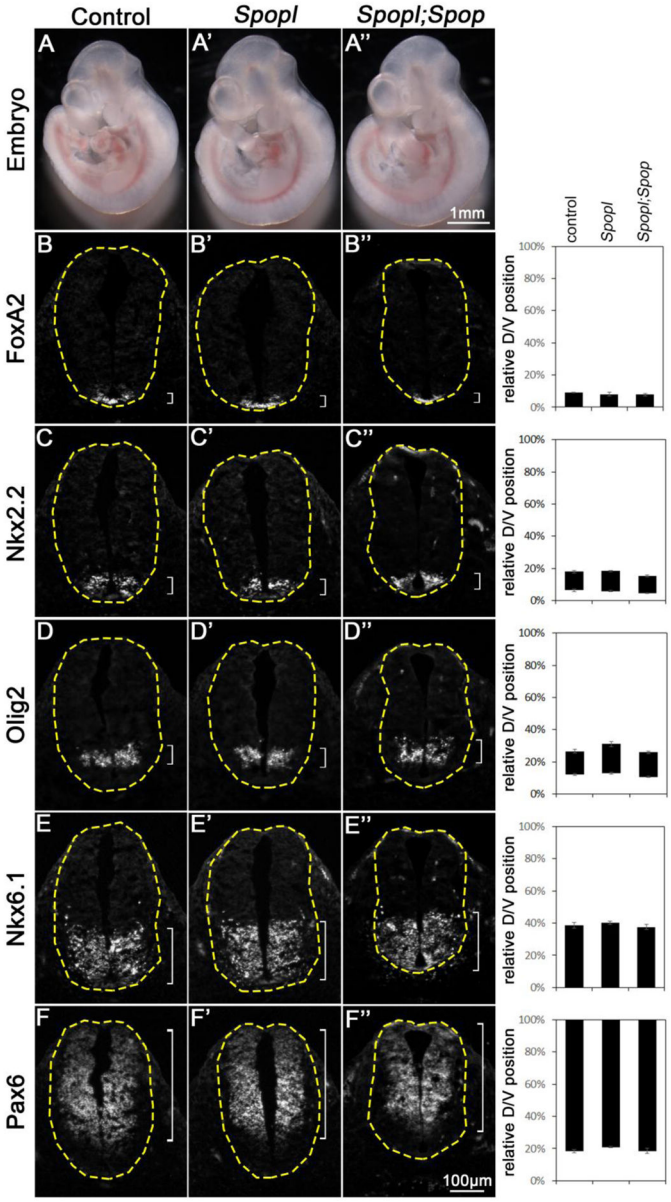

Fig. 3. Normal ventral patterning of the *Spopl* mutant and *Spopl;Spop* double mutant spinal cords

(A–A″) Lateral views of E10.5 control (A), *Spop* mutant (A′) and *Spopl;Spop* double mutant (A″) embryos. (B–F″) Immunofluorescent images of transverse sections of E10.5 control (n=4 embryos), *Spopl* mutant (n=4 embryos) and *Spopl;Spop* double mutant (n=4 embryos) spinal cords at the forelimb level with indicated antibodies are shown. The spinal cords are outlined with dash lines. Brackets indicate the expression domains. The span of each domain along the D/V axis is quantified and shown on the right. Relative D/V position is shown as the distance to the ventral-most point of the spinal cord as a percentage of the entire D/V span of the spinal cord. Student's *t*-test suggests no significant difference between *Spopl;Spop* double mutant, *Spopl* mutant and control groups. The morphology and

spinal cord neural patterning of both *Spopl* mutant and *Spopl;Spop* double mutant resemble wild type.

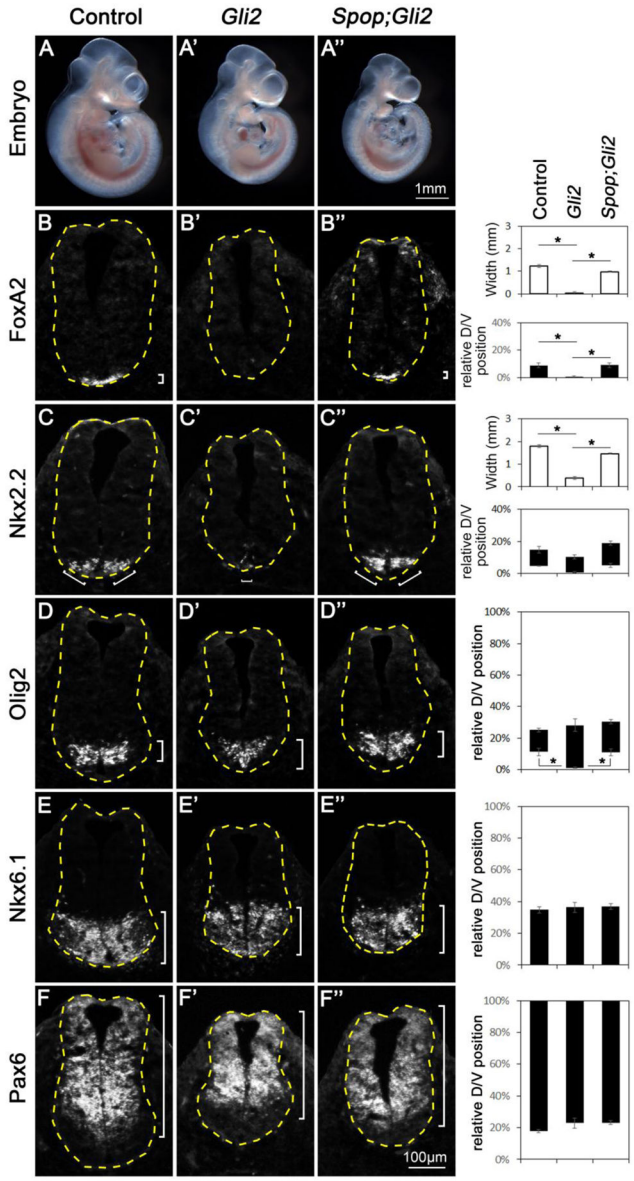

Fig. 4. Restored floor plate and V3 interneuron progenitor fates in *Spop;Gli2* double mutants

(A–A″) Lateral views of E10.5 control (A), *Gli2* mutant (A′) and *Spop;Gli2* double mutant (A″) embryos. (B–F″) Immunofluorescent images of transverse sections of E10.5 control (n=3 embryos), *Gli2* mutant (n=3 embryos) and *Spop;Gli2* (n=3 embryos) double mutant spinal cords at the forelimb level with indicated antibodies. The spinal cords are outlined with dash lines. Brackets indicate the expression domains. The span of each domain along D/V axis is shown on the right. Relative D/V position is shown as the distance to the ventral-most point of the spinal cord as a percentage of the entire D/V span of the spinal cord. The width of *Foxa2* and *Nkx2.2* domains is also quantified (hollow columns). (B–B″) *Foxa2* was present in the ventral-most region of the control and diminished in the *Gli2* mutant, but restored in the *Spop;Gli2* double mutant spinal cords. Student's *t*-test was employed to compare the width of floor plate. *: $p<0.05$. (C–C″) *Nkx2.2* was present in juxtaposition to

floor plate of the control but diminished in the *Gli2* mutant, and was restored in the *Spop;Gli2* double mutant spinal cords. Student's *t*-test was employed to compare the size of V3 interneuron progenitor domain. *: $p<0.05$. (D–D″) *Olig2* expression was excluded from the ventral-most region of control and *Spop;Gli2* double mutant but expanded ventrally in *Gli2* mutant spinal cords. Student's *t*-test was employed to compare the distance from the *Olig2* expression domain to the ventral-most point of the spinal cords. *: $p<0.05$. (E–F″) *Nkx6.1* and *Pax6* expression domains remained unchanged in the *Gli2* mutant and *Spop;Gli2* double mutant spinal cords.

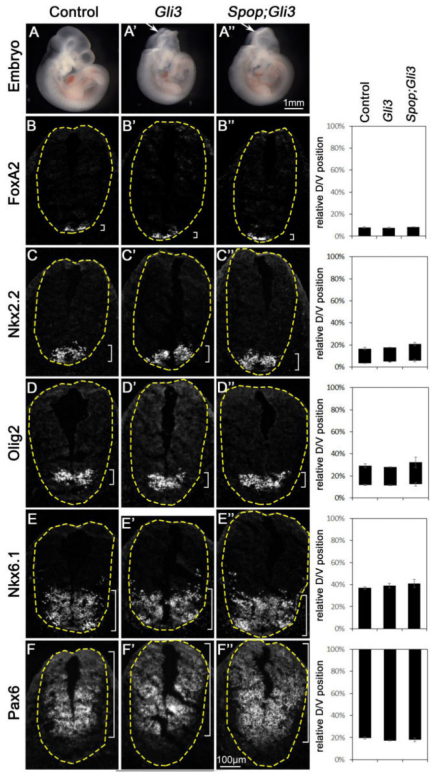

Fig. 5. *Spop;Gli3* double mutants resembled *Gli3* mutants in ventral spinal cord patterning

(A–A″) Lateral views of E10.5 control (A), *Gli3* mutant (A′) and *Spop;Gli3* double mutant (A″) embryos. Arrows in A′ and A″ indicate exencephaly. (B–F″) Immunofluorescent images of transverse sections of E10.5 spinal cords in *Gli3* mutant (n=4 embryos) and *Spop;Gli3* double mutant (n=5 embryos) resembled those in the control (n=5 embryos) at the forelimb level with indicated antibodies. The spinal cords are outlined with dash lines. Brackets indicate the expression domains. The span of each domain is quantified and shown on the right. Relative D/V position is shown as the distance to the ventral-most point of the spinal cord as a percentage of the entire D/V span of the spinal cord. Student's *t*-test suggests no significant difference between *Spop;Gli3* double mutant, *Gli3* mutant and control groups.

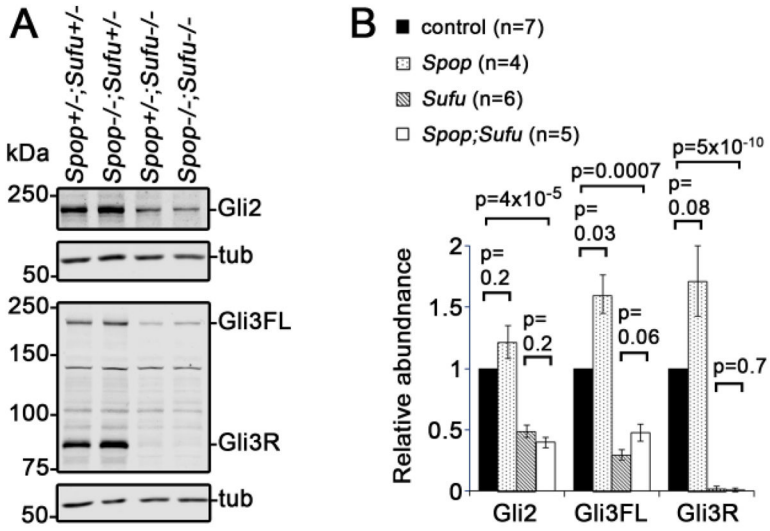

Fig. 6. Moderate increase in the level of Gli3, but not Gli2, in *Spop;Sufu* double mutant embryos

(A) Immunoblots of E9.5 embryo lysates with indicated antibodies. (B) Quantitative analyses of the levels of Gli2, Gli3FL and Gli3R (normalized to β-tubulin, mean ± SEM) based on the data of immunoblot analyses. Statistical significance was determined with Student's *t*-test.

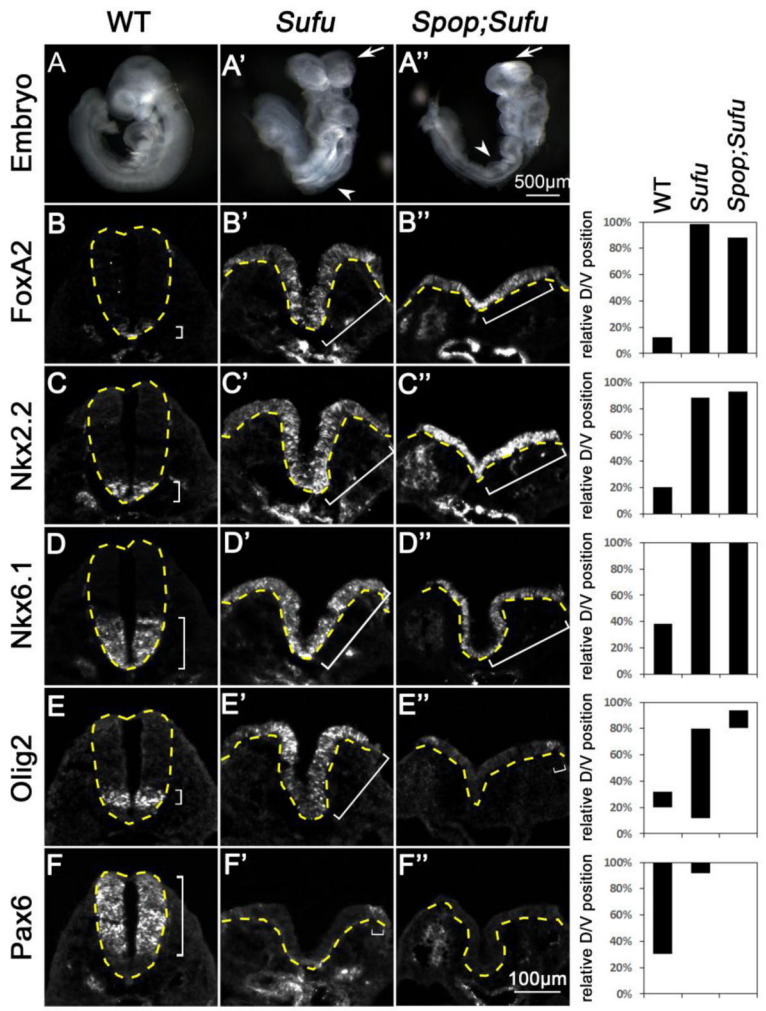

Fig. 7. Loss of *Spop* exacerbated the ventralization of the *Sufu* mutant spinal cord

(A–C) Lateral views of E9.5 wild type (A), *Sufu* mutant (A′) and *Spop;Sufu* double mutant (A″) embryos. Arrows in B and C indicate exencephaly; arrowheads indicate spina bifida. (B–F″) Immunofluorescent images of transverse sections of E9.5 spinal cords at the thoracic level. The spinal cords are outlined with dash lines. Brackets indicate the expression domains. (B–C″) *Foxa2* and *Nkx2.2* were expressed in the ventral-most region of wild type but expanded to the dorsal region in the *Sufu* mutant and *Spop;Sufu* double mutant spinal cords. (D–D″) *Nkx6.1* expression domain was expanded to the dorsal region in both *Sufu* mutant and *Spop;Sufu* double mutant spinal cords. (E–E″) *Olig2* expression was shifted to the dorsal region in *Sufu* mutant and even more dorsally shifted in *Spop;Sufu* double mutant spinal cords. (F–F″) *Pax6* expression domain was shifted dorsally in *Sufu* mutant and was absent in *Spop;Sufu* double mutant spinal cord. n=2 embryos for each genotype were analyzed. The span of each domain is quantified and shown on the right. Relative D/V position is shown as the distance to the ventral-most point of the spinal cord as a percentage of the entire D/V span of the spinal cord.

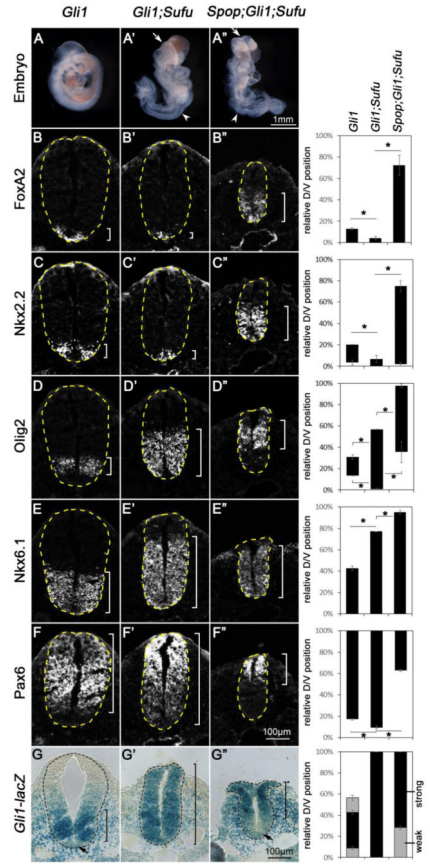

Fig. 8. Loss of *Spop* rescued the floor plate and V3 interneuron progenitor fates in *Gli1;Sufu* double mutant embryos

(A–A″) Lateral views of E9.5 *Gli1* mutant (A), *Gli1;Sufu* double mutant (A′) and *Spop;Gli1;Sufu* triple mutant (A″) embryos. Arrows in A′ and A″ indicate exencephaly; white arrowheads indicate spina bifida; red arrowheads indicate edema. (B–G″) Immunofluorescent (B–F″) or Xgal-stained (G–G″) images of transverse sections of the E9.5 *Gli1* mutant (n=3 embryos), *Gli1;Sufu* double mutant (n=3 embryos) and *Spop;Gli1;Sufu* triple mutant (n=3 embryos) spinal cords at the thoracic level. The spinal cords are outlined with dash lines. Brackets indicate the expression domains. The span of each domain along the D/V axis is shown on the right. Relative D/V position is shown as the distance to the ventral-most point of the spinal cord as a percentage of the entire D/V span of the spinal cord. Student's *t*-tests were performed to compare the dorsal and ventral borders of expression domains of various genes. *: $p<0.05$. (B–C″) The expression of *Foxa2* and *Nkx2.2* in the ventral-most region of *Gli1* mutant was diminished in *Gli1;Sufu* double mutant, but expanded dorsally in the *Spop;Gli1;Sufu* triple mutant spinal cords. (D–D″) *Olig2* expression was expanded both ventrally and dorsally in *Gli1;Sufu* double mutant, but was dorsally restricted in the *Spop;Gli1;Sufu* triple mutant spinal cords. (E–E″) *Nkx6.1* expression domain was expanded dorsally in the *Gli1;Sufu* double mutant and more dorsally in the *Spop;Gli1;Sufu* triple mutant spinal cords. (F–F″) *Pax6* expression domain was expanded ventrally in the *Gli1;Sufu* double mutant, and restricted to the more dorsal region in the *Spop;Gli1;Sufu* triple mutant spinal cord. (G) *Gli1-lacZ* expression formed a ventral-

to-dorsal gradient in the *Gli1* mutant spinal cord, with the exception of the floor plate, in which *Gli1-lacZ* has been downregulated. (G′) Strong *Gli1-lacZ* expression is present throughout the entire spinal cord of *Gli1;Sufu* double mutant. (G″) *Gli1-lacZ* is highly expressed in the dorsal, but not ventral region of the *Spop;Gli1;Sufu* triple mutant spinal cords.

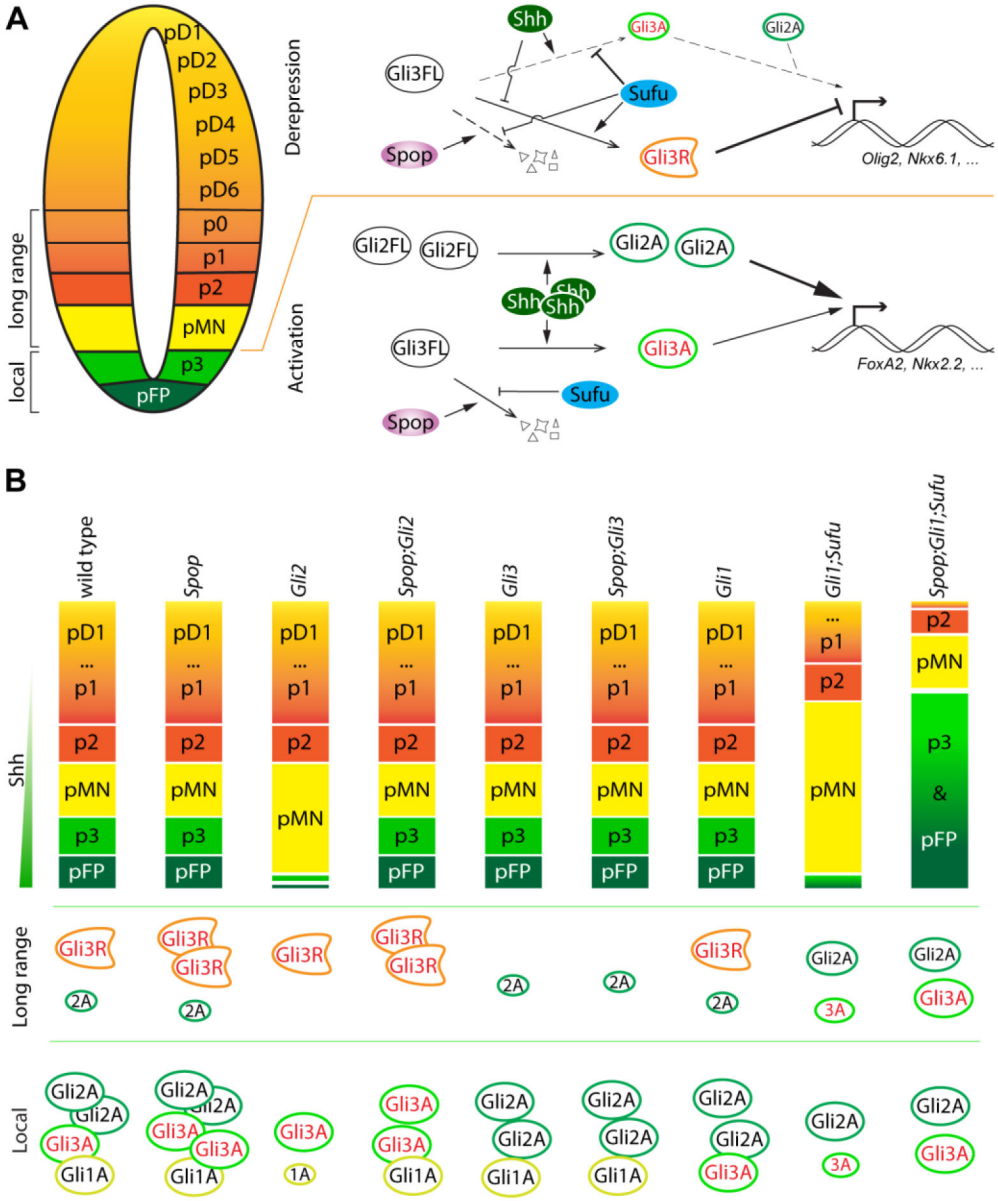

Fig. 9. A model of the roles of Spop in spinal cord patterning

(A) In the lateral region of the spinal cord (long range) including p0-pMN, low to intermediate levels of Shh reduce the production of Gli3R from Gli3FL by antagonizing the repressive function of Sufu, allowing the expression of genes such as *Olig2* and *Nkx6.1*. In pFP and p3, high levels of Shh promote the production of Gli2A and Gli3A, which then activate the expression of *Foxa2* and *Nkx2.2*. Gli2A plays a more predominant role than Gli3A in this context. Spop targets Gli3 for degradation, preventing over activation of the Shh pathway. (B) The levels of both Gli3A and Gli3R increase in the absence of Spop, but the effect of the increased Gli3A on the formation of pFP and p3 is only revealed in *Spop;Gli2* double mutants, in which the much more potent Gli2A is absent. In *Gli1;Sufu* double mutants, the reduced levels of Gli2A and Gli3A are insufficient to support pFP and p3 formation. Loss of *Spop* increases Gli3A and rescues the formation of pFP and p3 in

Sufu;Gli1;Spop triple mutants. The moderate increase in Gli3R in the absence of *Spop* does not show apparent effect in ventral spinal cord patterning in various single and compound mutants.